Preprints of the 21st IFAC World Congress (Virtual)
Berlin, Germany, July 12-17, 2020

Thermal Monitoring of Buildings by Aggregated Temperature Estimation ⋆

Muhammad Umar B. Niazi * **Carlos Canudas-de-Wit** *
Alain Y. Kibangou *

* *Univ. Grenoble Alpes, CNRS, Inria, Grenoble INP, GIPSA-Lab, 38000 Grenoble, France, (email: muhammad-umar-b.niazi@gipsa-lab.fr, carlos.canudas-de-wit@gipsa-lab.fr, alain.kibangou@univ-grenoble-alpes.fr).*

Abstract: Thermal monitoring is important not only to ensure the comfort of building inhabitants but also to reduce energy consumption and greenhouse gas emissions. It can be, however, a challenging task because of limited computational and sensing resources at hand. This paper provides an efficient technique to estimate average (or mean operative) temperatures of rooms in a building. The proposed average observer is of minimum order whose parameters are chosen to minimize the asymptotic estimation error. The results show the effectiveness of the approach in the estimation-based temperature regulation.

Keywords: Building thermal model, average temperature observer, optimal estimation.

1. INTRODUCTION

Residential and commercial buildings play a significant part in global energy consumption and greenhouse gas emissions. For instance, in France, they are one of the largest sources of energy consumption, Lévy and Belaïd (2018), and amount to 23% of the national greenhouse gas emissions, Derbez et al. (2014). In mitigating the effects of global warming, therefore, one of the forefronts is to develop efficient techniques for thermal monitoring and control of the buildings.

Model-based techniques are considered to be quite effective in thermal monitoring and control of buildings, Oldewurtel et al. (2010) and Maasoumy et al. (2013). In particular, resistor-capacitor (RC) network models offer an exceptional balance between simplicity and accuracy, Bueno et al. (2012) and Ramallo-González et al. (2013). However, such models are not tractable because they scale badly with the size of a building and require a tremendous amount of computational and sensing equipment. To deal with this issue, Deng et al. (2014) presented a model reduction technique to reduce the dimension of the building thermal model. It provides an aggregated thermal representation of the building elements. Such a representation, although optimal for model reduction, may not be favorable for monitoring. This is because the aggregated parts, for instance, may consist of several walls in the building that are not directly linked with each other.

In this paper, we provide a design of an average observer that considers pre-specified aggregated thermal elements, which are called clusters, and estimates their average temperatures. Each cluster is meaningful and comprises the elements (or nodes) of a certain room, i.e., air, internal mass, and inner envelope. The average temperatures represent the mean operative temperatures of rooms, which is considered to be a good measure for thermal comfort; Boduch and Fincher (2009). For each cluster, average deviation is assumed to be small due to the diffusive nature of heat and the fact that the nodes in each cluster are connected, thus allowing heat flow among themselves.

We consider the 4-room building setup of Deng et al. (2014) and obtain an optimal estimate of average temperatures of the rooms. That is, the design matrices of the average observer are chosen such that the estimation error is minimum. This is achieved by optimizing a single parameter in a convex minimization problem, which simplifies the problem to a great degree.

The rooms are heated by a simple on/off control policy that takes the estimate of the average temperatures as a feedback. The performance of the proposed observer is satisfactory with the mean estimation error of about 2% (approximately $\pm 0.4\,^{\circ}\mathrm{C}$). Moreover, since the estimation error is small, the on/off controller is able to regulate the mean operative temperatures of rooms in the comfortable range of 20-22 °C, Burroughs and Hansen (2004).

2. BUILDING THERMAL MODEL

There is a duality between heat transfer and electrical phenomenon, Skadron et al. (2002), where the temperature difference is analogous to voltage, heat flow to current, thermal resistance to electrical resistance, and thermal mass to electrical capacitance. Therefore, resistor-capacitor (RC) network models are considered to be suitable for the heat conduction. Convection and radiation, on the other hand, can be approximated by a resistor with a nominal empirical resistance value; Mathews et al. (1994).

⋆ This work is supported by European Research Council (ERC) under the European Union's Horizon 2020 research and innovation programme, ERC-AdG no. 694209, Scale-FreeBack (Website: http://scale-freeback.eu/).

2.1 Model and parameters

We use the model of Wang and Xu (2006a), where the building envelope is represented by 3R2C shown in Fig. 1(c) and the internal mass by 2R2C shown in Fig. 1(b). The building envelope consists of the walls, ceiling, and floor, and the internal mass consists of the carpet, furniture, and people. The mean air temperature of the room is denoted as x_{in} in the figure. The heater model is shown in Fig. 1(a), where q_h is a known input and x_h is the temperature at the surface of a heater.

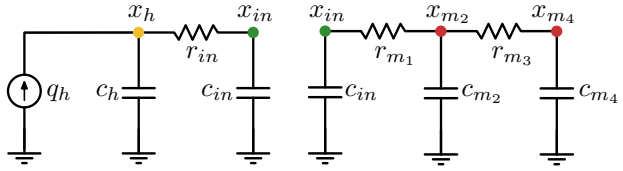

(a) Heater (b) 2R2C – Internal mass

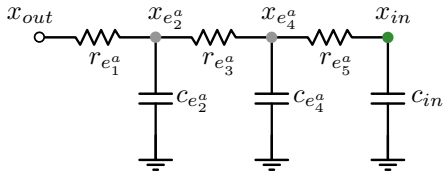

(c) 3R2C – Building envelope

Fig. 1. The elements of the building thermal model.

In Fig. 1(b), x_{m_2} is the mean surface temperature of the total mass and x_{m_4} is the mean temperature of its core. In Fig. 1(c), $x_{e_2^a}$ is the mean temperature of the outside of envelope-a and $x_{e_4^a}$ is the mean temperature of the inside of envelope-a, where a denotes a wall, ceiling, or floor. By employing the Kirchoff's current law, we find that the temperature x_i at node i is governed by

$$c_i \frac{dx_i}{dt} = \sum_{j \in \mathcal{N}_i} \frac{x_j - x_i}{r_{ij}} + \sum_k b_{ik} q_k, \tag{1}$$

where c_i is the capacitance of node i, $\mathcal{N}_i$ is the set of i's neighboring nodes, r_{ij} is the resistance between i and j, $b_{ik} \in \{0, 1\}$ is a scalar, and q_k is the heater input to i when $b_{ik} = 1$. The outside temperature x_{out} directly influences the room's temperature if it has a window; let r_w be the resistance that the window offers.

Table 1. Parameter values.

3R2C model	$r_{e_1^a}$	$c_{e_2^a}$	$r_{e_3^a}$	$c_{e_4^a}$	$r_{e_5^a}$
Ceiling	0.3	0.17	4	0.22	0.3
Floor	0.3	0.17	4	0.22	0.3
External walls	0.3	0.17	4	0.22	0.3
Internal walls	0.3	0.22	4	0.22	0.3
2R2C model	r_{m_1}	c_{m_2}	r_{m_3}	c_{m_4}	-
Internal mass	0.16	0.5	3	0.5	-

The parameter values for the 3R2C and 2R2C models are given in Table 1, where the resistance is measured in $\mathrm{m^2KW^{-1}}$ and the capacitance in $\mathrm{MJm^{-2}K^{-1}}$. The temperature is measured in K, which is converted to °C. We use the parameter values for 3R2C as provided in Deconinck and Roels (2016). The parameter values of 2R2C model are hypothetical because they depend on the type and quantity of internal mass of each room; Wang and Xu (2006b) provide an algorithm to identify these parameters. Furthermore, the resistance of a window $r_w = 3$ and the resistance from a heater to a room $r_{in} = 0.05$, whereas the capacitance of a room $c_{in} = 0.1$ and of a heater $c_h = 0.5$.

2.2 Building setup

We consider the 4-room building setup of Deng et al. (2014) shown in Fig. 2(a), whose RC-network representation is given in Fig. 2(b). In Deng et al. (2014), the internal mass of the rooms is neglected and the outside air is considered as a state node with a very large capacitance. Here, we consider internal mass and heaters in the rooms that adds 12 additional nodes to the network of Deng et al. (2014), which has 37 nodes. Also, we consider the outside temperature x_{out} as an input, and not a state, since it influences the building temperature and not vice versa. This subtracts one node from the network. Thus, we have 48 nodes in the RC-network as shown in Fig. 3. An arrow on some nodes represents an input at those nodes; all the black arrows indicate the outside temperature x_{out} and each yellow arrow indicates a heater input q_{h_p}, where $p = 1, 2, 3, 4$. Notice that, in Fig. 2(b) and Fig. 3, there is an edge from the inner floor node to the outer internal mass node.

We assume that the four heater nodes are the *measured* nodes, that is, the temperature evolution on the surface of the heaters is measured by the sensors. The remaining nodes in the system are called *unmeasured* nodes.

2.3 State-space representation

To provide the state-space representation, we index the nodes as follows. Nodes corresponding to the outside of the building envelope are $\mathcal{V}_o = \{1, 2, \cdots, 12\}$. Unmeasured nodes corresponding to the four rooms are $\mathcal{V}_{r_1} = \{13, 14, \cdots, 20\}$, $\mathcal{V}_{r_2} = \{21, 22, \cdots, 28\}$, $\mathcal{V}_{r_3} = \{29, 30, \cdots, 36\}$, and $\mathcal{V}_{r_4} = \{37, 38, \cdots, 44\}$, respectively. Measured nodes, which are the heaters' surfaces, are $\mathcal{V}_h = \{45, 46, 47, 48\}$. Let $i = 1, 2, \cdots, 48$. Then, the temperature of node i at time $t \geq 0$ is denoted as $x_i(t) \in \mathbb{R}$. Thus, the state vector $\mathbf{x} = [\, x_1 \ \cdots \ x_{48} \,]^\top$ and the state-space representation of the system is

$$\mathbf{\Sigma} : \begin{cases} \dot{\mathbf{x}}(t) = A\mathbf{x}(t) + B\mathbf{u}(t) \\ \mathbf{y}(t) = C\mathbf{x}(t), \end{cases} \tag{2}$$

where $\mathbf{u} = [\, q_{h_1} \ q_{h_2} \ q_{h_3} \ q_{h_4} \ x_{out} \,]^\top$ is the input vector and $\mathbf{y} = [\, x_{45} \ x_{46} \ x_{47} \ x_{48} \,]^\top$ is the output vector.

The system's structure is represented by a (bidirected) graph $\mathcal{G} = (\mathcal{V}, \mathcal{E}, \mathcal{W})$ shown in Fig. 3, where

$$\mathcal{V} = \mathcal{V}_o \cup \mathcal{V}_{r_1} \cup \mathcal{V}_{r_2} \cup \mathcal{V}_{r_3} \cup \mathcal{V}_{r_4} \cup \mathcal{V}_h$$

is the set of nodes, $\mathcal{E} \subset \mathcal{V} \times \mathcal{V}$ is the set of edges, and

$$\mathcal{W} = \left\{ \frac{1}{c_i r_{ij}} : (i, j) \in \mathcal{E} \right\}$$

is the set of edge weights. The graph is bidirected because the edge weight for $(i, j) \in \mathcal{E}$ is $(c_i r_{ij})^{-1}$, whereas the edge weight for $(j, i) \in \mathcal{E}$ is $(c_j r_{ij})^{-1}$. Thus, the off-diagonal entries of the state matrix A, for $i \neq j$, are given as

$$[A]_{ij} = \begin{cases} (c_i r_{ij})^{-1}, & \text{if } (i, j) \in \mathcal{E}, \\ 0, & \text{otherwise;} \end{cases}$$

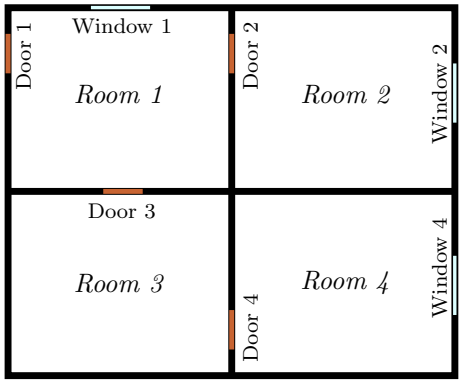

(a) Building envelope reproduced from Deng et al. (2014)

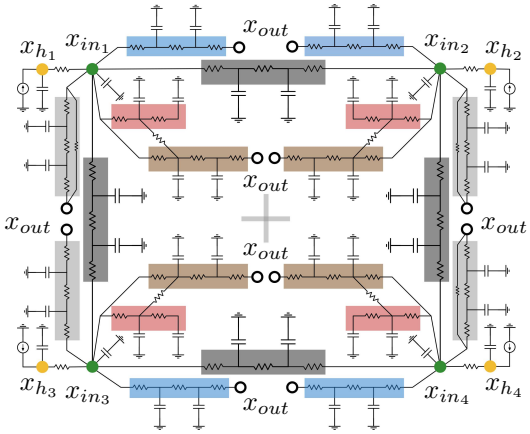

(b) RC-network representation of the building

Fig. 2. RC network model of the building setup in (a). In (b), the colored rectangular blocks correspond to ceiling (blue), floor (brown), outer walls (light gray), inner walls (dark gray), and internal mass (red). The windows are represented by resistors in parallel to the 3R2C models of walls.

and the diagonal entries are given as

$$[A]_{ii} = \begin{cases} -(r_{ii})^{-1} - \sum_{j \neq i} [A]_{ij}, & \text{if } i \in \mathcal{S}_o, \\ -\sum_{j \neq i} [A]_{ij}, & \text{if } i \in \mathcal{V} \setminus \mathcal{S}_o; \end{cases}$$

where $\mathcal{S}_o = \mathcal{V}_o \cup \{13, 21, 37\}$ is the set of nodes directly influenced by the outside temperature x_{out}. Here, c_i is the capacitance of the node i and r_{ij} is the resistance between node i and j; also, $r_{ii} = r_{e_1^a}$, if $i \in \mathcal{V}_o$, and $r_{ii} = r_w$, if $i \in \{13, 21, 37\}$.

The output matrix $C = [\, 0_{4\times 44} \;\; I_4 \,]$ and the input matrix

$$[B]_{ip} = \begin{cases} (c_i r_{ii})^{-1}, & \text{if } i \in \mathcal{S}_o \text{ and } p = 5, \\ 1, & \text{if } (i,p) = \{(13,1),(21,2),(29,3),(37,4)\}, \\ 0, & \text{otherwise.} \end{cases}$$

3. PROBLEM DEFINITION

The goal is to estimate temperature evolution of some thermal elements, which can be useful in temperature regulation of a building. We remark that the system $\mathbf{\Sigma}$ is not observable because the observability matrix

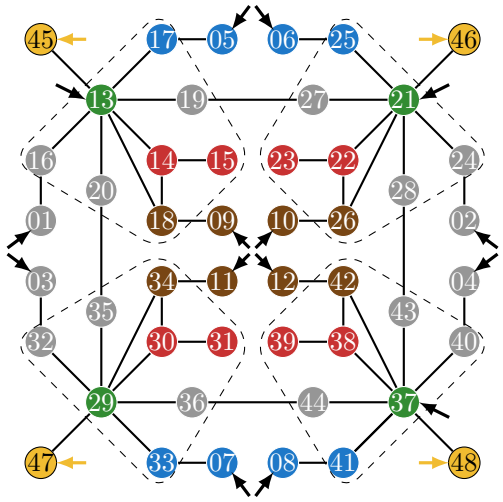

Fig. 3. System's graph with 48 nodes and 52×2 edges, where the green nodes represent the rooms, the red nodes represent the internal mass, the blue nodes represent the ceiling, the brown nodes represent the floor, the gray nodes represent the walls, and the yellow nodes represent the heaters. The four yellow arrows represent inputs from the four heaters, whereas all the black arrows represent the input x_{out}. The temperature at the heater nodes is measured. The clusters of unmeasured nodes corresponding to each room are encircled by a dashed line.

$\mathcal{O} = [\, C^\top \;\; (CA)^\top \;\; \cdots \;\; (CA^{47})^\top \,]^\top$ has a rank deficiency, i.e., $\operatorname{rank} \mathcal{O} = 40 < 48$. The system is unobservable due to the graph structure in Fig. 3, and not due to the specific parameters. This implies that the full state reconstruction of $\mathbf{\Sigma}$ is impossible.

Placing additional sensors to make the system observable is not only uneconomical but also computationally expensive, because the full state reconstruction requires an observer of order equal to the system's dimension, which could be very large if the building is large. Also, knowledge of the full state may be unnecessary for the temperature regulation. In general practice, the temperature of the room is regulated by doing a feedback from the air temperature measurements of the rooms. However, the air temperature is not a valid measure for assessing thermal comfort of the room.

In this paper, we consider each room along with the nodes that represent its internal mass and inner envelope. This forms *clusters* of nodes $\mathcal{V}_{r_1}, \mathcal{V}_{r_2}, \mathcal{V}_{r_3}, \mathcal{V}_{r_4}$ that are encircled by a dashed line in Fig. 3. Our aim is to estimate the average temperature of each cluster, known as the mean operative temperature of the room, which is considered to be a good measure of thermal comfort, Boduch and Fincher (2009).

Let $\mathbf{x} = [\, \mathbf{x}_1^\top \;\; \mathbf{x}_2^\top \,]^\top$, where $\mathbf{x}_1 = [\, x_1 \;\cdots\; x_{44} \,]^\top$ and $\mathbf{x}_2 = [\, x_{45} \;\cdots\; x_{48} \,]^\top$ are the states of the unmeasured and the measured nodes, respectively. With such a partition, we have the following partition of the systems matrices:

$$A = \begin{bmatrix} A_{11} & A_{12} \\ A_{21} & A_{22} \end{bmatrix}, \; B = \begin{bmatrix} B_1 \\ B_2 \end{bmatrix}, \; C = [\, 0_{4\times 44} \;\; I_4 \,].$$

The average states (mean operative temperatures) corresponding to $\mathcal{V}_{r_1}, \mathcal{V}_{r_2}, \mathcal{V}_{r_3}, \mathcal{V}_{r_4}$ clusters are

$$x_1^{\text{av}} = \frac{1}{8}\sum_{i=13}^{20} x_i, \quad x_2^{\text{av}} = \frac{1}{8}\sum_{i=21}^{28} x_i,$$
$$x_3^{\text{av}} = \frac{1}{8}\sum_{i=29}^{36} x_i, \quad x_4^{\text{av}} = \frac{1}{8}\sum_{i=37}^{44} x_i.$$

In addition, we also consider $\mathcal{V}_o$ cluster of outer envelope nodes, whose average state is $x_0^{\text{av}} = \frac{1}{12}\sum_{i=1}^{12} x_i$. Here, we assume the average to be average mean, however, it can be generalized to any weighted average. The dynamics of the averages are given by the projected system

$$\mathring{\boldsymbol{\Sigma}} : \begin{cases} \dot{\mathbf{z}}(t) = E\mathbf{z}(t) + F\boldsymbol{\sigma}(t) + G\mathbf{u}(t) \\ \mathbf{y}(t) = H\mathbf{z}(t) \\ 0 = Q^\top \boldsymbol{\sigma}(t), \end{cases} \tag{3}$$

where $\mathbf{z} = [\, x_0^{\text{av}} \; x_1^{\text{av}} \; \cdots \; x_4^{\text{av}} \; \mathbf{x}_2^\top \,]^\top$ and

$$E = \begin{bmatrix} \Lambda Q^\top A_{11} Q & \Lambda Q^\top A_{12} \\ A_{21} Q & A_{22} \end{bmatrix}, \quad F = \begin{bmatrix} \Lambda Q^\top A_{11} \\ A_{21} \end{bmatrix},$$
$$H = \begin{bmatrix} 0_{4\times 5} & I_4 \end{bmatrix}, \quad G = \begin{bmatrix} \Lambda Q^\top B_1 \\ B_2 \end{bmatrix}.$$

Here, $Q = \text{diag}[\, \mathbf{1}_{12}, \mathbf{1}_8, \mathbf{1}_8, \mathbf{1}_8, \mathbf{1}_8 \,]$, and $\Lambda = (Q^\top Q)^{-1}$. Note that $\boldsymbol{\sigma} = [\, \boldsymbol{\sigma}_0^\top \; \boldsymbol{\sigma}_1^\top \; \boldsymbol{\sigma}_2^\top \; \boldsymbol{\sigma}_3^\top \; \boldsymbol{\sigma}_4^\top \,]^\top$ is the vector of deviations of the states of each cluster from its average state, i.e., $\boldsymbol{\sigma} := J\mathbf{x}$ with $J = [\, I_{44} - Q\Lambda Q^\top \; 0_{44\times 4} \,]$.

Problem statement. Given a building thermal model $\boldsymbol{\Sigma}$ with temperature measurements $\mathbf{y}(t)$ at measured nodes, estimate the mean operative temperatures $x_1^{\text{av}}(t)$, $x_2^{\text{av}}(t)$, $x_3^{\text{av}}(t)$, $x_4^{\text{av}}(t)$ of the rooms.

4. MULTI-CLUSTER AVERAGE ESTIMATION

In this section, we first provide the multi-cluster average observer whose design matrices depend on an arbitrary matrix V. We find the explicit solution V^* such that the effect of average deviation of clusters on the estimation is minimized. Finally, we formulate the minimization problem in terms of the asymptotic estimation error. The decision variable of the problem is $\alpha > 0$ such that $V = \alpha V^*$ minimizes the asymptotic estimation error.

4.1 Multi-cluster average observer

We provide the design of a multi-cluster average observer, which is the extension of a single cluster average observer given in Niazi et al. (2020). The difficulty in dealing with multiple clusters arises due to the coupling between the clusters. The observer, which is of minimum order and is similar to Darouach (2000), is given by:

$$\boldsymbol{\Omega}^{\text{av}} : \begin{cases} \dot{\mathbf{w}}(t) = M\mathbf{w}(t) + K\mathbf{y}(t) + NG\mathbf{u}(t) \\ \hat{\mathbf{z}}^{\text{av}}(t) = \mathbf{w}(t) + L\mathbf{y}(t), \end{cases} \tag{4}$$

where $\mathbf{w}(t), \hat{\mathbf{z}}^{\text{av}}(t) \in \mathbb{R}^5$ and the matrices M, K, N, L are of appropriate dimensions. Let the estimation error be

$$\boldsymbol{\zeta} := \mathbf{z}^{\text{av}} - \hat{\mathbf{z}}^{\text{av}},$$

where $\mathbf{z}^{\text{av}} = [\, x_0^{\text{av}} \; x_1^{\text{av}} \; \cdots \; x_4^{\text{av}} \,]^\top$ is the vector of average states of clusters and $\hat{\mathbf{z}}^{\text{av}} = [\, \hat{x}_0^{\text{av}} \; \hat{x}_1^{\text{av}} \; \cdots \; \hat{x}_4^{\text{av}} \,]^\top$ is the vector of estimated average states. From (3) and (4), we obtain

$$\begin{aligned} \dot{\boldsymbol{\zeta}}(t) &= (E_{11} - LE_{21})\boldsymbol{\zeta}(t) + (E_{11} - LE_{21})(\mathbf{w}(t) + L\mathbf{y}(t)) \\ &\quad - M\mathbf{w}(t) + (E_{12} - K - LE_{22})\mathbf{y}(t) \\ &\quad + (F_1 - LF_2)\boldsymbol{\sigma}(t) + (G_1 - LG_2 - NG)\mathbf{u}(t), \end{aligned}$$

where $E_{11} = \Lambda Q^\top A_{11} Q$, $E_{12} = \Lambda Q^\top A_{12}$, $E_{21} = A_{21}Q$, $E_{22} = A_{22}$, $F_1 = \Lambda Q^\top A_{11}$, $F_2 = A_{21}$, $G_1 = \Lambda Q^\top B_1$, and $G_2 = B_2$. From this equation, we see that it is critical to minimize the influence of $\boldsymbol{\sigma}$ on the estimation error $\boldsymbol{\zeta}$. Since $Q^\top \boldsymbol{\sigma} \equiv 0$ by definition, therefore we choose L according to $F_1 - LF_2 = VQ^\top$, for some V defined subsequently. Thus,

$$\begin{aligned} L &= -(VQ^\top - \Lambda Q^\top A_{11})A_{21}^+ \\ N &= [\, I_5 \quad -L \,] \\ M &= NFQ \\ K &= \Lambda Q^\top A_{12} + ML - LA_{22}, \end{aligned} \tag{5}$$

where $V \in \mathbb{R}^{5\times 5}$ is such that $M = \Lambda Q^\top A_{11} Q + (VQ^\top - \Lambda Q^\top A_{11})A_{21}^+ A_{21} Q$ is Hurwitz. Here, A_{21}^+ is the Moore-Penrose inverse of A_{21}. Given a matrix V, the solution L in (5) is the minimizing solution to $|||F_1 - LF_2 - VQ^\top|||$, see Campbell and Meyer (2009), where $|||\cdot|||$ is a matrix norm induced by Euclidean norm. With (5), it directly follows that

$$\dot{\boldsymbol{\zeta}}(t) = M\boldsymbol{\zeta}(t) + NF\boldsymbol{\sigma}(t). \tag{6}$$

4.2 Influence of average deviation

The estimation error $\boldsymbol{\zeta}$ doesn't converge to zero due to the influence of the average deviation vector $\boldsymbol{\sigma}$ in the error dynamics (6). We would like to minimize this influence, i.e., $\min \|NF\boldsymbol{\sigma}(t)\|$, where $\|\cdot\|$ is the Euclidean norm and N is given in (5) that depends on the choice of V.

Because of the diffusive nature of heat and the connectivity of clusters, we remark that $\|\boldsymbol{\sigma}(t)\|$ is not only bounded for all $t \geq 0$, but also it is small. Therefore, it makes sense to provide an optimal design of multi-cluster average observer $\boldsymbol{\Omega}^{\text{av}}$. Consider the design matrices L, N as in (5), which depend on the matrix V, then we have the following:

Proposition 1. The solution to the minimization problem

$$\min_V \|N_V F\boldsymbol{\sigma}(t)\| \tag{7}$$

is $V^* = \Lambda Q^\top A_{11} Q\Lambda$, where $N_V = N$ as given in (5).

Proof. If there exists a matrix V such that $N_V F = VQ^\top$, then $N_V F\boldsymbol{\sigma} = 0$. Therefore, V must be chosen such that $|||N_V F - VQ^\top|||$ is minimized. Thus, (7) is equivalent to

$$\min_V |||N_V F - VQ^\top|||.$$

Note that $N_V F - VQ^\top = F_1 - L_V F_2 - VQ^\top$, where $L_V = L$ as in (5). Expanding the right hand side of this equation gives

$$(\Lambda Q^\top A_{11} - VQ^\top)(I - A_{21}^+ A_{21}).$$

From this expression, we see that $V = \Lambda Q^\top A_{11} Q\Lambda$ is the optimal solution to (7). □

The solution V^* in Proposition 1 minimizes the exogenous signal $NF\boldsymbol{\sigma}$ in (6). However, it is not the optimal solution in terms of the estimation of average temperatures of clusters. This is due to (i) it may not minimize $\limsup_{t\to\infty} \|\boldsymbol{\zeta}(t)\|$, which also depends on M, and (ii) it may not ensure that $M = NFQ$ is Hurwitz.

4.3 Error minimization

The asymptotic estimation error is $\limsup_{t\to\infty}\|\boldsymbol{\zeta}(t)\|$, which we aim to minimize. We choose $V = \alpha V^*$, where $\alpha \in \mathbb{R}$ is the decision variable of the minimization problem and V^* is given in Proposition 1. The constraint to this minimization problem is to choose α such that

$$M = \Lambda Q^\top A_{11}\left(I - (I - \alpha Q\Lambda Q^\top)A_{21}^+ A_{21}\right)Q, \qquad (8)$$

from (5), is Hurwitz. By expanding the right hand side, we see that one part

$$\Lambda Q^\top A_{11}(I + \alpha Q\Lambda Q^\top)A_{21}^+ A_{21}Q$$

is Hurwitz if $\alpha \geq 0$, because it is a Metzler matrix with dominant diagonal values. The other part $-\Lambda Q^\top A_{11}A_{21}^+ A_{21}Q$ is not Hurwitz by the same argument. Combining this with the fact that $V \neq 0$, we choose the domain $\alpha > 0$ that must be explored to make M Hurwitz.

Suppose M is Hurwitz, then, from the solution trajectory of (6), we have

$$\begin{aligned}
&\limsup_{t\to\infty}\|\boldsymbol{\zeta}(t)\| = \limsup_{t\to\infty}\left\|\int_0^t \exp(M\tau)NF\boldsymbol{\sigma}(t-\tau)d\tau\right\| \\
&= \limsup_{t\to\infty}\left\|\int_0^t \exp(M\tau)(NF - VQ^\top)\boldsymbol{\sigma}(t-\tau)d\tau\right\| \\
&\leq \limsup_{t\to\infty}\left\|\int_0^t \exp(M\tau)(NF - VQ^\top)d\tau \cdot \mathbf{1}\sup_{0\leq\theta\leq t}\|\boldsymbol{\sigma}(\theta)\|\right\|,
\end{aligned}$$

where $\mathbf{1}$ is the vector of ones with appropriate dimension. The term $\sup_{0\leq\theta\leq t}\|\boldsymbol{\sigma}(\theta)\|$ cannot be minimized since it depends on the dynamics of the system $\boldsymbol{\Sigma}$. Therefore, we postulate the cost functional to minimize $\limsup_{t\to\infty}\|\boldsymbol{\zeta}(t)\|$ as follows:

$$\begin{aligned}
\min_{\alpha>0}\quad & \left\|\int_0^\infty \exp(M_\alpha\tau)(N_\alpha F - \alpha V^* Q^\top)d\tau\right\| \qquad (9)\\
\text{s.t.}\quad & M_\alpha \text{ is Hurwitz},
\end{aligned}$$

where $M_\alpha = M$ is in (8), V^* is given in Proposition 1, and

$$N_\alpha = \begin{bmatrix} I_5 & (\alpha V^* Q^\top - \Lambda Q^\top A_{11})A_{21}^+ \end{bmatrix}.$$

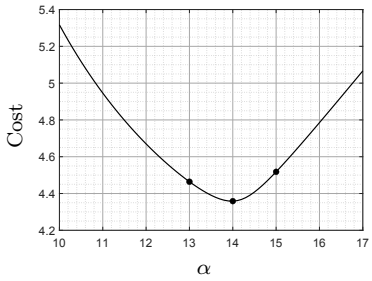

Fig. 4. Cost functional in (9) versus α. The minimum is achieved at $\alpha = 14$ for the building setup of Fig. 2.

The problem (9) can be solved by a simple greedy algorithm, which can be summarized as follows:

(i) Increase α until M_α is Hurwitz.
(ii) Repeat iteration: At each iteration, with a small step $\epsilon > 0$, increase $\alpha \leftarrow \alpha + \epsilon$ and compute the cost (9).
(iii) Stop iteration when a (local) minimum is reached.

For the building setup of this paper, the cost functional in (9) is convex and the solution is found to be $\alpha^* = 14$, as shown in Fig. 4.

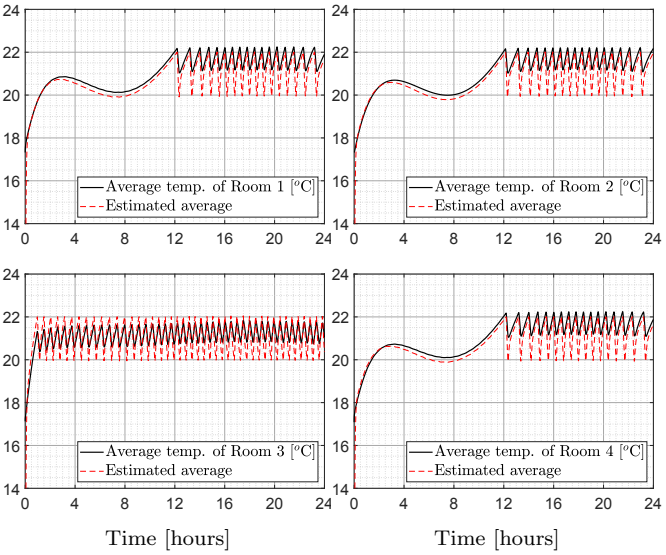

Fig. 5. Average temperature estimation of the rooms in a building.

5. RESULTS AND DISCUSSION

We implement the multi-cluster average observer $\boldsymbol{\Omega}^{\text{av}}$ for the building setup of Section 2. The initial conditions $\mathbf{x}(0) \in \mathbb{R}^{48}$ of $\boldsymbol{\Sigma}$ are chosen randomly in the interval $(10, 20)$. The output $\mathbf{y}(t)$ of the system consists of the temperature measurements at the heaters' surfaces. The input $\mathbf{u} = [\,\mathbf{u}_h^\top \;\; x_{out}\,]^\top$, where $\mathbf{u}_h^\top = [\,q_{h_1} \;\; q_{h_2} \;\; q_{h_3} \;\; q_{h_4}\,]$ is the input of the heaters and x_{out} is the known outside temperature. We suppose $x_{out}(t) = 5\sin(\pi/12\,t - \pi)$.

A simple on/off control policy is used for the heaters by taking a feedback of the estimates of rooms' mean operative temperatures from $\boldsymbol{\Omega}^{\text{av}}$. That is, the heater j turns on with $q_{h_j}(t, \hat{x}_j^{\text{av}}) = 50$ when $\hat{x}_j^{\text{av}}(t) \leq 20$, and it turns off with $q_{h_j}(t, \hat{x}_j^{\text{av}}) = 0$ when $\hat{x}_j^{\text{av}}(t) \geq 22$, where $j = 1, 2, 3, 4$. Inside the interval $20 < \hat{x}_j^{\text{av}}(t) < 22$, the control input $q_{h_j}(t, \hat{x}_j^{\text{av}})$ retains its value. That is, suppose $\hat{x}_j^{\text{av}}(t_1) \leq 20$, then, for $t > t_1$, the heater turns on with $q_{h_j}(t, \hat{x}_j^{\text{av}}) = 50$. When the heater is on, the mean operative temperature of room j starts to rise, and so does its estimate, i.e., $20 < \hat{x}_j^{\text{av}}(t) < 22$. The heater will stay on until $\hat{x}_j^{\text{av}}(t) = 22$, where it will be turned off. It will remain off, and the mean operative temperature falls and so does its estimate, until $\hat{x}_j^{\text{av}}(t)$ touches its lower limit of 20 °C, where the heater will be turned on again.

We compute $V = \alpha\Lambda Q^\top A_{11}Q\Lambda$, where $\alpha = 14$,

$$V = \begin{bmatrix}
-24.59 & 0.64 & 0.64 & 0.64 & 0.64 \\
0.50 & -45.72 & 0.25 & 0.25 & 0 \\
0.50 & 0.25 & -45.72 & 0 & 0.25 \\
0.50 & 0.25 & 0 & -44.99 & 0.25 \\
0.50 & 0 & 0.25 & 0.25 & -45.72
\end{bmatrix},$$

then we compute L, N, M, K from (5). The plots of average temperatures of the rooms and their estimated trajectories are shown in Fig. 5. With a simple on/off control policy and an average observer, notice that average (or mean operative) temperatures of the rooms remain inside the thermal comfort range 20-22 °C. This comfort range is nominal but it can be adjusted according to weather,

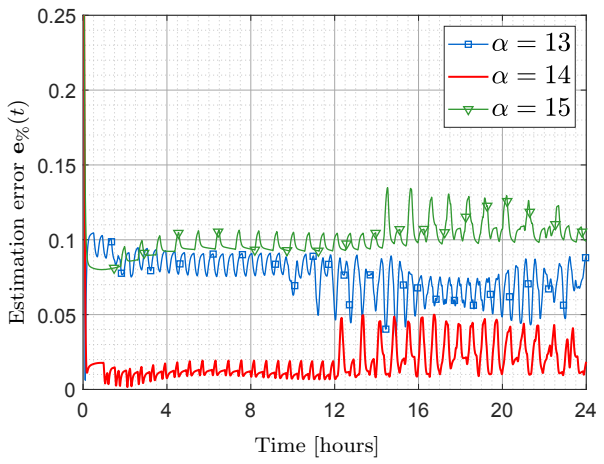

Fig. 6. Percentage estimation error for different α's.

building type, etc. In Fig. 5, notice that the average temperature of Room-3 reaches inside this range quickly because it doesn't have a window, therefore, it has a smaller influence of the outside temperature.

Let $\mathbf{z}_1^{\text{av}} = [\, x_1^{\text{av}} \;\; x_2^{\text{av}} \;\; x_3^{\text{av}} \;\; x_4^{\text{av}} \,]^\top$ and $\hat{\mathbf{z}}_1^{\text{av}} = [\, \hat{x}_1^{\text{av}} \;\; \hat{x}_2^{\text{av}} \;\; \hat{x}_3^{\text{av}} \;\; \hat{x}_4^{\text{av}} \,]^\top$. Then, the percentage estimation error $\mathbf{e}_{\%}(t)$ is defined as

$$\mathbf{e}_{\%}(t) = \frac{\|\mathbf{z}_1^{\text{av}}(t) - \hat{\mathbf{z}}_1^{\text{av}}(t)\|}{\|\mathbf{z}_1^{\text{av}}(t)\|}.$$

The performance of $\mathbf{\Omega}^{\text{av}}$ is quite satisfactory as shown in Fig. 6. For the optimal value $\alpha = 14$, the mean percentage error is 2.08%, i.e., around 0.4 °C for the range 20-22 °C, and the maximum percentage error is 4.9%, i.e., around 1 °C for the range 20-22 °C.

In conclusion, we presented an observer that estimates the mean operative temperatures of rooms in a building with minimum error. The dimension of the proposed observer equals the number of rooms (or clusters) plus one, where the extra 'one' is due to the cluster of nodes representing outer envelope of the building. The problem of error minimization is simplified to a great degree by formulating it with respect to a single parameter α, whose optimal value is found by a greedy algorithm. We employed a simple on/off control policy based on the average observer to regulate the mean operative temperatures of rooms. Such on/off policy for regulation saves around 25.32% of the energy, which means that the heaters on average remain off 25.32% of the day. The goal of this paper was estimation, the development of a better control technique to further minimize the energy consumption is deferred for the future work.

REFERENCES

Boduch, M. and Fincher, W. (2009). Standards of human comfort: relative and absolute. URL `http://hdl.handle.net/2152/13980`.

Bueno, B., Norford, L., Pigeon, G., and Britter, R. (2012). A resistance-capacitance network model for the analysis of the interactions between the energy performance of buildings and the urban climate. *Building and Environment*, 54, 116–125.

Burroughs, H. and Hansen, S.J. (2004). *Managing indoor air quality*. The Fairmont Press, Inc.

Campbell, S.L. and Meyer, C.D. (2009). *Generalized inverses of linear transformations*. SIAM.

Darouach, M. (2000). Existence and design of functional observers for linear systems. *IEEE Transactions on Automatic Control*, 45(5), 940–943.

Deconinck, A.H. and Roels, S. (2016). Comparison of characterisation methods determining the thermal resistance of building components from onsite measurements. *Energy and Buildings*, 130, 309–320.

Deng, K., Goyal, S., Barooah, P., and Mehta, P.G. (2014). Structure-preserving model reduction of nonlinear building thermal models. *Automatica*, 50(4), 1188–1195.

Derbez, M., Berthineau, B., Cochet, V., Lethrosne, M., Pignon, C., Riberon, J., and Kirchner, S. (2014). Indoor air quality and comfort in seven newly built, energy-efficient houses in France. *Building and Environment*, 72, 173–187.

Lévy, J.P. and Belaïd, F. (2018). The determinants of domestic energy consumption in France: Energy modes, habitat, households and life cycles. *Renewable and Sustainable Energy Reviews*, 81, 2104–2114.

Maasoumy, M., Moridian, B., Razmara, M., Shahbakhti, M., and Sangiovanni-Vincentelli, A. (2013). Online simultaneous state estimation and parameter adaptation for building predictive control. In *ASME 2013 Dynamic Systems and Control Conference*, volume 2.

Mathews, E., Richards, P., and Lombard, C. (1994). A first-order thermal model for building design. *Energy and Buildings*, 21(2), 133–145.

Niazi, M.U.B., Deplano, D., Canudas-de-Wit, C., and Kibangou, A.Y. (2020). Scale-free estimation of the average state in large-scale systems. *IEEE Control Systems Letters*, 4(1), 211–216.

Oldewurtel, F., Parisio, A., Jones, C.N., Morari, M., Gyalistras, D., Gwerder, M., Stauch, V., Lehmann, B., and Wirth, K. (2010). Energy efficient building climate control using stochastic model predictive control and weather predictions. In *Proceedings of the 2010 American Control Conference*, 5100–5105.

Ramallo-González, A.P., Eames, M.E., and Coley, D.A. (2013). Lumped parameter models for building thermal modelling: An analytic approach to simplifying complex multi-layered constructions. *Energy and Buildings*, 60, 174–184.

Skadron, K., Abdelzaher, T., and Stan, M.R. (2002). Control-theoretic techniques and thermal-RC modeling for accurate and localized dynamic thermal management. In *Proceedings Eighth International Symposium on High Performance Computer Architecture*, 17–28.

Wang, S. and Xu, X. (2006a). Simplified building model for transient thermal performance estimation using GA-based parameter identification. *International Journal of Thermal Sciences*, 45(4), 419–432.

Wang, S. and Xu, X. (2006b). Parameter estimation of internal thermal mass of building dynamic models using genetic algorithm. *Energy conversion and management*, 47(13-14), 1927–1941.